PLASTICITY AND RESISTANCE INDICES IN Cu/SOFT SUBSTRATE AND Cu/HARD SUBSTRATE COATED SYSTEMS

DARIA GRABCO[1], CONSTANTIN PYRTSAC[1,2], OLGA SHIKIMAKA[1]

[1] Institute of Applied Physics, MD-2028, Chisinau, Republic of Moldova
[2] Technical University of Moldova, MD-2004, Chisinau, Republic of Moldova
E-mail: daria.grabco@ifa.md, grabco@mail.ru

Received October 25, 2022

Abstract. This work, deals with the effect of various Cu/LiF, Cu/MgO, and Cu/Si coated systems on the change in the plasticity index H/E and the resistance index H^3/E^2 under indentation in a wide range of loads P_{max} = 5–900 mN. The main parameters of elasticity, strength and plasticity were determined, as well as the values of H/E and H^3/E^2. The general and specific features of the coated systems deformation under the action of a concentrated load were revealed. The deformation structure of the coated systems was examined at the dislocation level, which made it possible to establish the response mechanism of the CSs to the action of an external load and to explain the specific nature of the plastic and strength properties of the composite systems of "soft film/soft substrate" and "soft film/hard substrate" types.

Key words: Coated systems, Cu/soft substrate, Cu/hard substrate, nanoindentation, mechanism, plasticity index, resistance index.

1. INTRODUCTION

The coated film/substrate type systems (CSs) are used extensively in modern nanotechnology. The areas of application of such structures are extremely diverse. Composite systems of a thin metal layer/substrate are used in micro/nanoelectronics for the production of integrated circuits, magnetic and optical devices, in the jewelry and tool industries, in medicine and aviation industry, etc. As a result, the CSs creation of different types becomes necessary.

Thus, in the semiconductor technology, when creating systems of micro/ nanoelectromechanical (MEMS) and (NEMS) devices, films from soft materials are grown on hard substrates that ensure the obtainment of the "soft film/hard substrate" type of structures. In other areas, the "soft film/soft substrate", "hard film/hard substrate", and "hard film/soft substrate" CSs types are used. In this case, the microstructure of thin films and their mechanical properties become critical parameters that determine the quality and service life of the manufactured products.

The mechanical properties improvement of MEMS/NEMS structures is often just as important as that of the opto-electric properties. The mechanical degradation of structures over time is a factor which affects the device mass production. The intensive development of nanotechnologies reduces film thickness to micro- and

nanometer sizes. During operation, these structures undergo natural wear, and the higher the degree of wear, the sooner the device breaks. Therefore, along with the new types of CSs creation, intensive work is underway to increase the durability of coatings. In the scientific literature [1–5], in order to assess the resistance of materials to plastic deformation and to evaluate the degree of wear, in addition to traditional parameters, hardness H and elastic modulus E, other characteristics are also used, namely, the "plasticity index" and "resistance index". These parameters characterize the material's resistance to deformation and fracture after the application of a concentrated external load and are defined as the ratio between the hardness and Young's modulus of the material, H/E and H^3/E^2, respectively.

Based on the observation of Tabor [6, 7] that the hardness of metals is usually 3 times as much as the yield strength, Johnson [8] estimated contact load P_y required to initiate the plastic deformation:

$$\boldsymbol{P}_y = 0.78\, r^2\, (H^3 / E^2), \tag{1}$$

here r is the radius of the sphere pressed against the elastic/plastic half-space; H and E, respectively, are the hardness and elastic modulus of the half-space. This equation shows that the resistance to the onset of the plastic deformation is higher in materials with larger H^3/E^2 values, *i.e.* in materials with high hardness and low modulus.

In [4], an assessment of the mechanical behavior of hard and superhard nanocomposite coatings measured by a computer-controlled microhardness tester was made. The authors showed that no clear relationship was between the mechanical response of the coating and separately between the values of H and E, but this response naturally depended on the parameters H/E and H^3/E^2: the plastic deformation was as higher, as higher H/E and lower H^3/E^2. In another work [3], the behavior of these parameters in phosphate glasses doped with rare earth elements was studied with an increase in the load on the indenter, and it was shown that both H/E and H^3/E^2 decrease with an increase in the load. This means that with the load increase, the plastic properties of phosphate glasses reduce, whereas the strength properties increase.

The published data clearly demonstrate that the H/E and H^3/E^2 parameters can be successfully used to evaluate the plastic, strength, brittle and tribological properties of various materials, both of bulk and coated systems, along with traditional parameters, hardness and Young's modulus. The evaluation of these parameters may be of a particular interest for Cu/substrate structures, which underlie a large number of (MEMS) and (NEMS) devices [9–12].

In our earlier works, the mechanical properties of the Cu/substrate type structures (Cu/LiF, Cu/MgO, Cu/Si) were studied thoroughly depending on the film thickness and the magnitude of the applied load under indentation [13–16]. Therefore, it seems extremely valuable for practice to compare the plastic, strength, and wear-resistant properties of these structures based on the same film material (Cu) but different types of chemical bonds in the substrates. In this regard, the effect of various

Cu/substrate systems (Cu/LiF, Cu/MgO, Cu/Si) on the change in the parameters H/E and H^3/E^2 under indentation with different loads will be studied in this work.

2. MATERIALS AND METHODS

A group of coated systems was chosen for the research, namely, Cu thin films deposited on various substrates. Single crystals with a gradual change in the type of atomic bonding were chosen as substrates: ionic crystal – LiF, ionic-covalent crystal MgO and covalent crystal Si. Crystals have different types of crystalline structure (LiF, MgO – NaCl type; Si – diamond type). Cu and LiF belong to soft materials with H = 0.6 and 1.2 GPa, while MgO and Si are hard crystals with H = 7.5 and 8.2 GPa, respectively. As a result, three groups of CSs were obtained depending on the type of substrate: 1 – 'soft film/soft substrate, ionic', SS_i (Cu/LiF), 2 – 'soft film/hard substrate', ionic-covalent, SH_{ic} (Cu/MgO) and 3 – 'soft film/hard substrate', covalent, SH_c (Cu/Si). For each type of substrates, similar composite structures were fabricated with the thickness of Cu films: t_1 = 85; t_2 = 470 and t_3 = 1000 nm. All structures were obtained under the same conditions. Cu films were deposited on a freshly prepared surface of single crystal substrates by magnetron sputtering, at a Magnetron Sputtering RF device, in the P = 200 W, T = 50°C mode.

The mechanical properties were studied using the depth-sensitive indentation method at a Nanotester-PMT3-NI-02 instrument equipped with a Berkovich indenter. The tests were carried out in the following mode: loading process – 20 s, exposure at a maximum load (P_{max}) – 30 s, and unloading – 20 s. Twelve maximum loads were used within P_{max} = (5–900) mN. For each load, 10 imprints were applied. The results were calculated as the average of 10 trials. The main parameters of elasticity, plasticity and strength were estimated based on the indentation curves' analyses. The calculations were performed automatically, using the instrument software according to the Oliver-Pharr method used extensively in science [17]. The surface microstructure was studied by optical microscopy (OM) using XJL-101, Amplival instruments, microinterferometer MII-4 and a Nanostation II atomic force microscope (AFM). To detect the contribution of the substrate to the deformation process, the Cu film was removed using a solution of 70% HNO_3 + 30% CH_3COOH, then an aqueous solution of $FeCl_3$ for LiF and the composition 5 pNH_4Cl + 1 pH_2O + 1 pH_2SO_4 for MgO were used to reveal dislocation structures.

3. RESULTS

To learn about the deformation specifics of the crystals chosen as substrates, Fig. 1 can be used, which shows the shape of the imprints and the surface topography in three sections for the (001) plane of LiF, MgO, and Si (100) single crystals. It can be seen from the presented images that in the given range of nano- and submicroloads, P = (20–200) mN, the imprints on all crystals are plastic, without any cracks and

fractures. Near the center of each of the three sides of the imprints, pile-ups are formed, indicating plastic displacement of the material onto the crystal surface. The high plasticity of these crystals in the range of loads up to 200 mN is also confirmed by the $P(h)$ curves both at the loading and unloading stages. As an example, Fig. 2 shows a series of curves obtained on LiF, MgO, Si substrate-crystals at different indenter loads, P_{max}, and, for comparison, $P(h)$ curves for polycrystalline copper, an initial component for the CSs films.

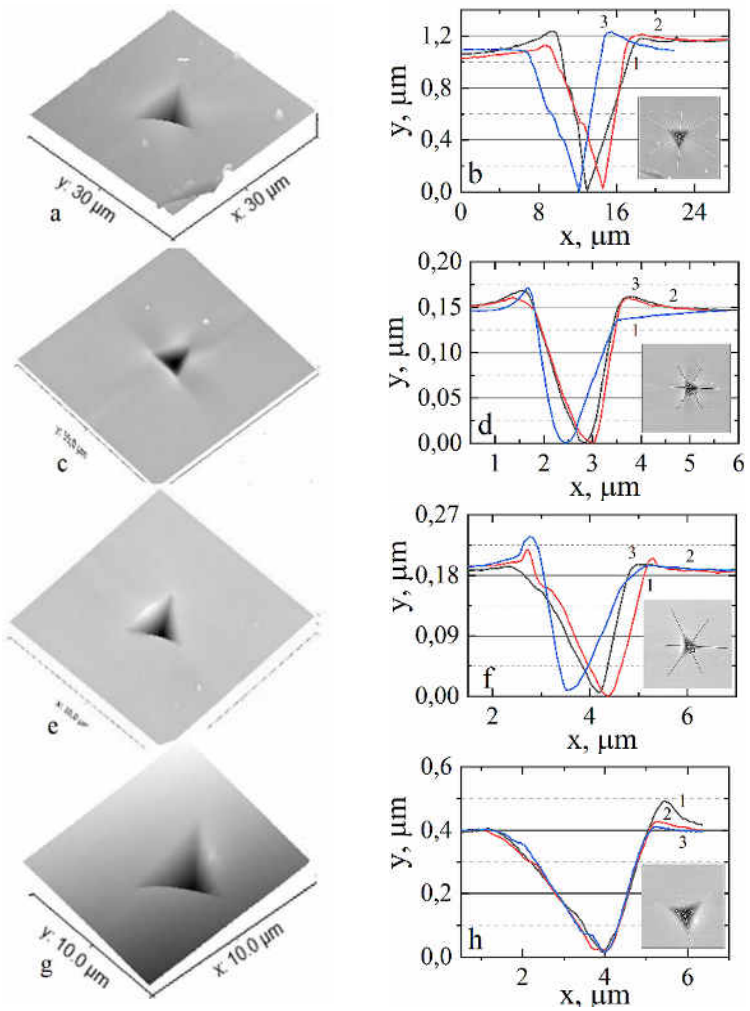

Fig. 1 – AFM – Surface nanostructure images, 3D looks of imprints (a,c,e,g) and profiles (b, d, f, h): (a, b) – LiF, P = 120 mN; (c, d) – MgO, P = 20 mN; (e, f) – Si, P = 30 mN; (g, h) – Si, P = 200 mN. The insertions in Figs. b, d, f, h show 2D image of imprints with indication of sections for the profiles.

It is seen that at loads P = 10–100 mN, the curves for Cu and LiF are smooth (Figs. 2a, 2b). The curves for MgO and Si also have a smooth course at the loading stage, while at the unloading stage, Si shows pop-out effects, which, as is known from the literature [18], are mainly due to the phase transitions (Fig. 2d).

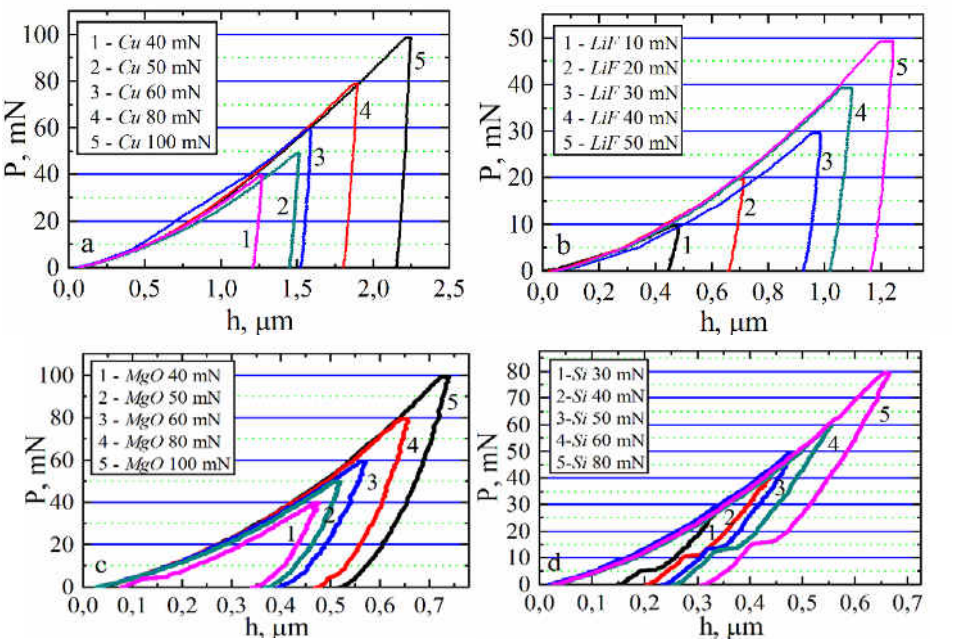

Fig. 2 – Deformation curves "load-indentation depth", $P(h)$, for Cu polycrystal, P = 40 – 100 mN, and monocrystals: LiF, P = 10 – 50 mN; MgO, P = 40 – 100 mN; Si, P = 30 – 80 mN.

Small pop-outs also occasionally appear in MgO crystals at the unloading stage, however, their appearance is usually associated with the rotational dislocation processes (Fig. 2c). There is another important difference observed in the indentation curves of the soft and hard crystals. In general, for Cu and LiF, a uniform character of the plastic deformation is observed with a slight elastic-plastic recovery at the stage of unloading. As for MgO and Si, a significant elastic-plastic recovery is observed here, and it is higher for Si than for MgO. In addition, as is described in [13–16], an increase in the load leads to a change in the process of deformation of the substrate crystals.

Several examples of the shape of indentations deposited on polycrystalline Cu and substrate-crystals under heavy loads are shown in Fig. 3. As follows from Fig. 3, the imprints on Cu and LiF are plastic, however, cracks and chips appeared near the imprints on MgO and Si. The difference in the behavior of substrate crystals under the action of an external load can also affect the tribological properties of all CSs, thereby changing their wear resistance. Estimation of the H/E

and H^3/E^2 parameters for the studied Cu/LiF, Cu/MgO and Cu/Si coated systems confirmed the above assumption (Figs. 4, 5).

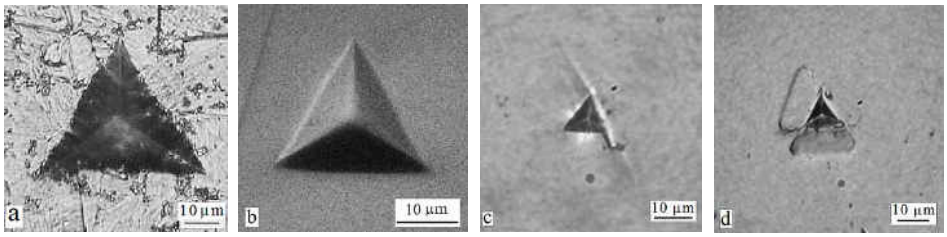

Fig. 3 – OM – Images of imprints obtained in reflection mode on the Cu polycrystal (a), and single crystals: LiF (b), MgO (c) and Si (d). *P* [mN]: a – 200; b – 300; c – 500; d – 700.

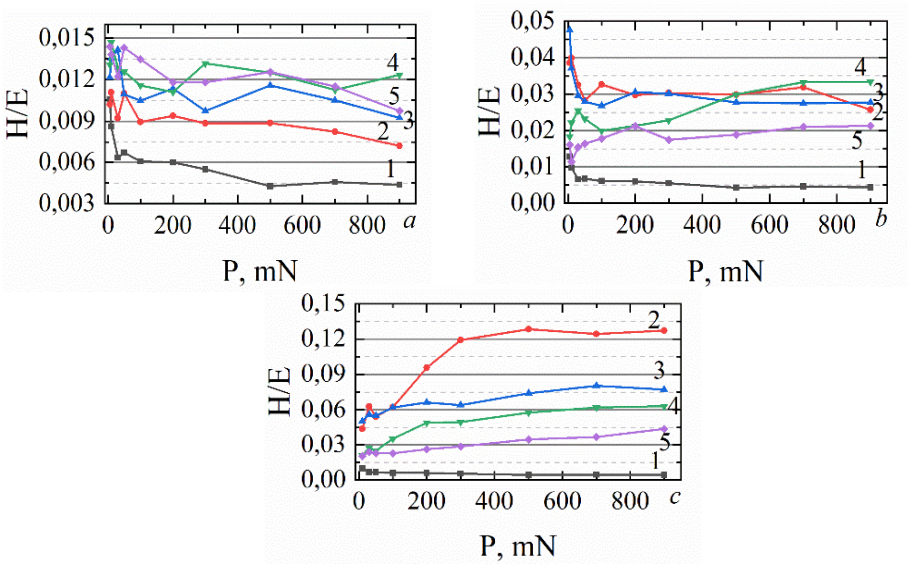

Fig. 4 – Typical curves reflecting the variations of the plasticity index *H*/*E* depending on the value of the P_{max} load at depth-sensing indentation in the range (5 – 900) mN for all CSs: a) – Cu/LiF, b) – Cu/MgO, c) – Cu/Si and the bulk crystals. The respective curves characterize: 1 – Cu polycrystal, 2 – LiF, MgO or Si monocrystals, 3 – Cu/substrate, t_1 = 85 nm, 4 – Cu/substrate, t_2 = 470 nm, 5 – Cu/substrate, t_3 = 1000 nm.

The values of the plasticity index *H*/*E* as a function of the load applied to the indenter under nano-microindentation, *H*/*E*(*P*), in the range of *P* = (5–900) mN are shown in Fig. 4. There is a following regularity that is traced. In general, all curves in Fig. 4a have a downward course with the load increasing, and the Cu-curve is the lowest of all. Curves of Cu/LiF CSs, 3–5, are at the top of the graph, above the LiF curve. This indicates that the plasticity of this composition has increased

compared to that of the original components, Cu and LiF. At the same time, the plasticity index of all samples decreases with the load increase. The curves of the next two graphs change regularly. Curve 3 – Cu/MgO CS (t = 85 nm) overlaps MgO curve (2), and as the film thickness increases, curves 4, 5 approach the Cu-curve. Also, the course of all CSs shows a tendency for saturation with the load increase (Fig. 4b). The effect of moving the Cu/Si curves away from the Si-curve and bringing them closer to Cu was even more evident in Fig. 4c. In addition, it can be seen that the curves tend to an increase. Changing the type of substrate leads to a change in the H/E value. So, when the load changes in the interval of P = (5–900) mN, the H/E value fluctuates within (0.009 – 0.015), (0.01–0.05), (0.02–0.075) for Cu/LiF CS, Cu/MgO CS and Cu/Si CS, respectively. Consequently, the H/E value for the same Cu film increases in the series of substrates: $SS_i < SH_{ic} < SH_e$.

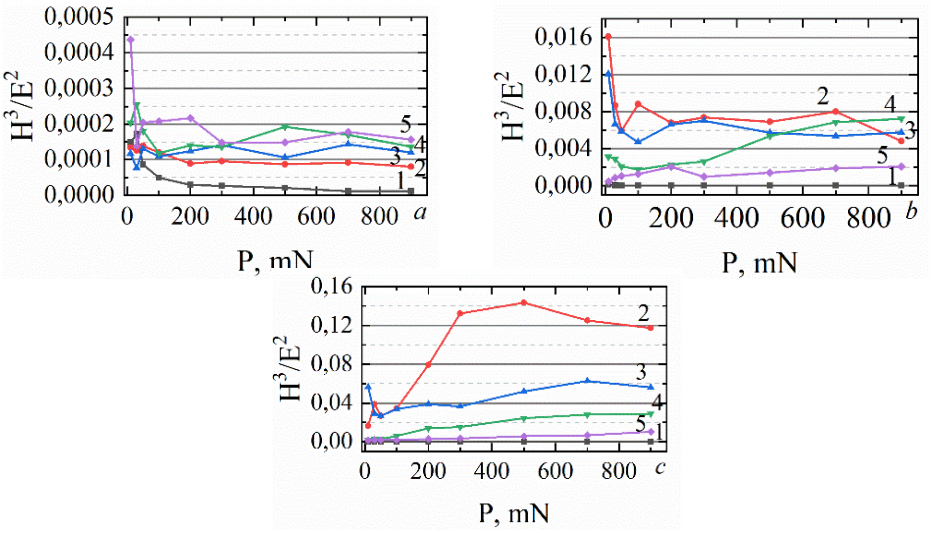

Fig. 5 – Typical curves reflecting the variations of the plasticity index H^3/E^2 depending on the value of the P_{max} load at depth-sensing indentation in the range (5 – 900) mN for all CSs: a) – Cu/LiF, b) – Cu/MgO, c) – Cu/Si and the bulk crystals. The respective curves characterize: 1 – Cu polycrystal, 2 – LiF, MgO or Si monocrystals, 3 – Cu/substrate, t_1 = 85 nm, 4 – Cu/substrate, t_2 = 470 nm, 5 – Cu/substrate, t_3 = 1000 nm.

Thus, the change in the substrate type leads to a regular change in the plastic properties of the coated system as a whole. Most likely, this is due to a similar change in the plasticity index H/E in a series of substrate crystals: $H/E_{LiF} < H/E_{MgO} < H/E_{Si}$ (see Fig. 4). A similar behavior was noted for the H^3/E^2 dependences of all studied CSs (Fig. 5). The SS_i curves are located higher than for Cu and LiF, while for SH_{ic} and SH_c the curves consecutively shift towards the Cu curve, more clearly for SH_c. However, although the CSs curves for the resistance index H^3/E^2 are located identically to the curves for the plasticity index H/E, the physical meaning

is the opposite. So, for example, an increase in the H/E parameter in Fig. 4a means an increase in plasticity, while an increase in the H^3/E^2 parameter (Fig. 5a) implies an increase in the resistance to plastic deformation for the CSs curves compared to the curves for Cu and LiF, *i.e.* decrease in plasticity. The reason for this effect will be discussed in the next section.

The transition to SH_{ic} and SH_c substrates is accompanied by a decrease in the H^3/E^2 parameter for all coated systems (CSs) compared to H^3/E^2_{MgO} and H^3/E^2_{Si}. In this case, the curve for CS_{1000nm} is the closest to the H^3/E^2_{Cu} curve, then the CS_{470nm} and CS_{85nm} curves consecutively approach the H^3/E^2_{MgO} and H^3/E^2_{Si} curves. Moreover, curves 3–5 in Fig. 5b are distributed evenly between curves 1 and 2, while curves 3–5 in Fig. 4c are close to curve 1, creating a large gap with curve 2 at loads $P > 100$ mN. As in the case of the H/E parameter, the change in the substrate type leads to a change in the value of H^3/E^2 for all the studied CSs and substrate crystals. When the load changes between P = (5 – 900) mN, the H^3/E^2 value fluctuates within (0.00007 – 0.00025), (0.0045 – 0.012), (0.01 – 0.06) for Cu/LiF CS, Cu/MgO CS and Cu/Si CS, respectively. The values of H^3/E^2 for the substrate crystals are distributed in the same order: LiF – (0.00008 – 0.00015), MgO – (0.0045 – 0.016), Si – (0.02 – 0.14). Thus, the value of H^3/E^2 for the same Cu film increases in the series of substrates: $SS_{Si} < SH_{ic} < SH_c$. The same is observed for the substrate crystals: $H^3/E^2_{LiF} < H^3/E^2_{MgO} < H^3/E^2_{Si}$ (Fig. 5). Thus, the obtained estimates demonstrated that in the case of the resistance index, as well as of the plasticity index, the change in the type of substrate leads to a regular change in the strength and tribological properties of the coated systems as a whole.

4. DISCUSSION

It is known at present [10, 19–21] that the CS hardness is a mechanical parameter that includes the hardness of the film and the hardness of the substrate. The ratio of these values gradually changes depending on the magnitude of the applied load. Along with this, when the indenter is deepened into the composite material, the structure and chemical composition of the deformable sample are changed. Thus, during the deformation of the soft-film/hard-substrate CS, the indenter penetrates into the film material easier, and after reaching the interface zone, it is more difficult to penetrate into the substrate material. Two factors, the film thickness, t, and the magnitude of the applied load, P_{max}, have a crucial effect on the course of this process. At the same time, their action has the opposite effect: the thicker the film, the longer the film material takes part in the deformation process, and later the substrate is included in the deformation process. And *vice versa*, the higher P_{max}, the deeper the indenter penetrates into the volume of the CS. As a result, the substrate material begins to make a greater contribution to the total deformation. The zone that separates the film material from the substrate material is referred to as the interface zone. When the indenter reaches the interface zone, the indentation

depth, h_{max}, becomes equal to the film thickness, t, and is denoted as $\beta = h_{max} / t = 1$, therefore, the greater the film thickness, the deeper the interface zone.

To elucidate the factors responsible for the characteristic course of the above H/E and H^3/E^2 curves, it seems important to estimate the maximum loads at which the indenter reaches the level of the interface zone on all studied CSs, polycrystalline copper, and LiF, MgO, and Si substrate crystals. The evaluation results are presented in Table 1.

Table 1

Maximum loads P_{max}, at which the indenter reaches the level of the interface zone $\beta = h_{max} / t \approx 1$ on all studied CSs, bulk Cu and substrate-crystals

Nr.	Sample	Cu, P_{max} [mN] for $h_{max} \approx t$	Crystal-substrate, P_{max} [mN] for $h_{max} \approx t$	P_{max} [mN] for CSs, $\beta = h_{max} / t \approx 1$	P_{max} CS / P_{max} subst.
1	2	3	4	5	6
1.	Cu/LiF, t = 85 nm	0.6	0.2	1.1	5.5
2.	Cu/LiF, t = 470 nm	10.5	12.0	7.5	0.71
3.	Cu/LiF, t = 1000 nm	30.0	40.0	35.0	0.88
4.	Cu/MgO, t = 85 nm	0.5	4.5	3.0	0.67
5.	Cu/MgO, t = 470 nm	10.0	45.0	25.0	0.56
6.	Cu/MgO, t = 1000 nm	30.0	180.0	100.0	0.56
7.	Cu/Si, t = 85 nm	0.5	5.0	5.0	1.0
8.	Cu/Si, t = 470 nm	10.0	43	27.0	0.63
9.	Cu/Si, t = 1000 nm	30.0	145.0	90.0	0.62

The load values at which the indenter reaches $h_{max} \approx t$ in polycrystalline copper and LiF crystal are close in magnitude (Table. 1). Due to this, in CSs of the SS_i type, the indenter reaches the level of the interface zone at loads close to P_{max} for Cu and for LiF. This means that the indenter passes easily from the film zone to the substrate zone without an additional deceleration. However, the situation changes for the SH_{ic} and SH_c structures. The loads at which the depth $h_{max} \approx t$ is reached are significantly higher for MgO and Si crystals than for Cu. In this regard, when the indenter reaches the interface zone, it undergoes deceleration on the part of MgO and Si crystals, to overcome which additional efforts are required. But ultimately the loads required to deepen the indenter to $\beta = h_{max}/t \approx 1$ in CSs turn out to be lesser than those for the substrate crystals due to the contribution of the soft film, which the indenter passes through with a lesser force (Table 1).

The proportion (P_{max} CS/P_{max} substrate) decreases with the film thickness increase, since the higher t, the greater part of the path the indenter passes in the film zone up to $\beta = h_{max}/t \approx 1$ (Table 1). A greater proportion of the film in the imprint formation process can affect the plastic and strength properties of the CS. This was

supported by the type of imprints. The imprints are deposited on Cu/LiF, Cu/MgO and Cu/Si CSs with different film thicknesses under the same load, P = 700 mN (Fig. 6). It can be seen that the largest and most plastic are the indentations on Cu/LiF CS. Only small brittle fractures appeared in the form of cracks and spalls near the indentations at CSs with t = 85 and 470 nm (Fig. 6 a-c). The degree of brittleness increases in the range of Cu/LiF-Cu/MgO-Cu/Si (Fig. 6a, 6d, 6g). With film thickness increase, t = 470 and 1000 nm, the brittle indentations became more ductile, and pile-ups appeared around them, most pronounced on Cu/LiF CS (Fig. 6b, 6c) and Cu/MgO CS (Fig. 6e, 6f). For greater clarity, the pile-up near an imprint (Fig. 6b) is shown in the interference mode in Fig. 6c.

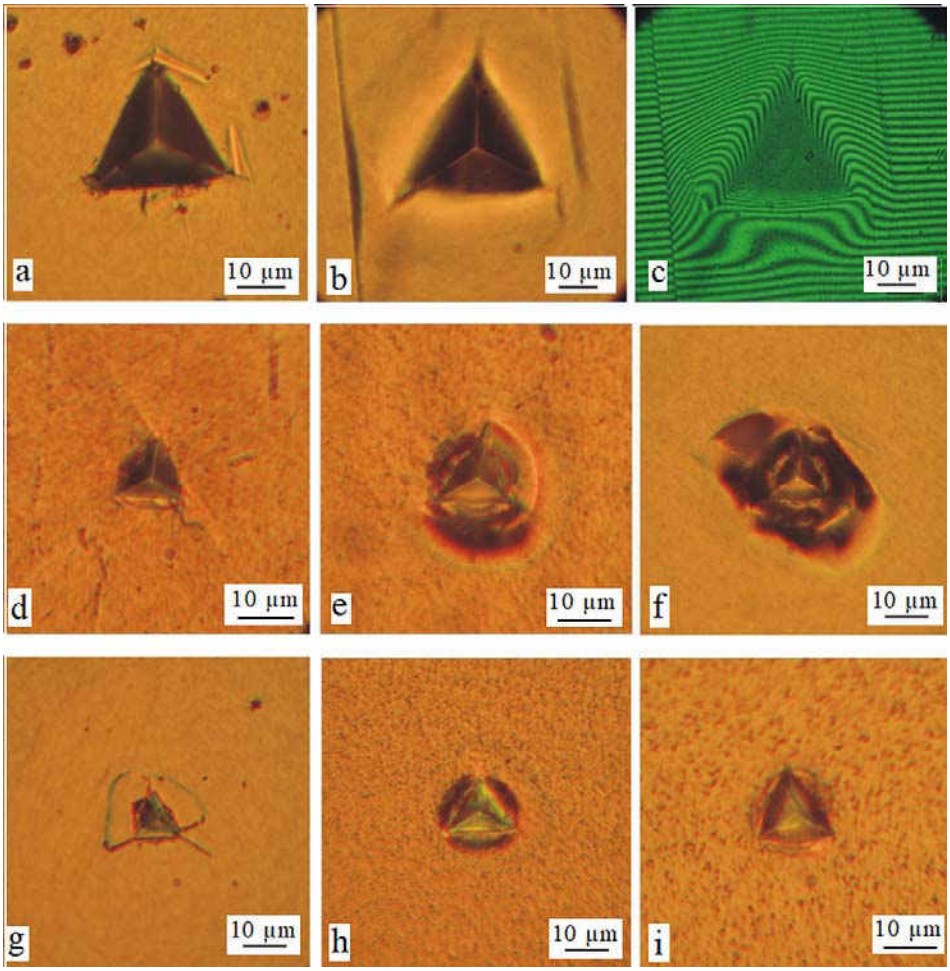

Fig. 6 – OM images of Berkovich imprints applied to the CSs: (a–c) – Cu/LiF; (d–f) – Cu/MgO; (g–i) – Cu/Si. (a, d, g) – t = 85 nm, (b, e, h) – t = 470 nm, (c, f, i) – t = 1000 nm. P = 700 mN. The imprint of Fig. 6b is demonstrated in the interference mode in Fig. 6c.

The difference in the shape and degree of the imprints' brittleness, depending on the type of substrate and the thickness of the Cu film, is observed not only on the surface of the coated systems, but also in the bulk of the samples after the film removal. As noted above, after overcoming the interface zone and with a continuing increase in the load, the indenter enters the substrate zone, forming imprints in it with the corresponding deformed zones around them. Dislocation rosettes appear in LiF and MgO substrate crystals, which can be visualized using the selective chemical etching after the Cu film removal. Figure 7a shows the dislocation rosette around the imprint on the LiF substrate after removing the copper film from the Cu/LiF_{85nm} CS and the type of dislocation rosettes after the LiF substrate surface slight polishing is presented in Figs. 7b, 7c.

It can be seen that the zone with a high dislocation density that has been formed near and under the imprints, is being gradually decreased when removed from the indentation. The creation of this zone is accompanied by mutual intersection of dislocations, dislocation-disclination clusters, and lattice rotation [22–24]. Similar processes also take place in other Cu/LiF and Cu/MgO CSs over a wide load range. In Cu/MgO CSs, due to a lower dislocation rate in MgO crystals than in LiF, the deformation zone is more packed, the dislocations are denser, which stimulates the formation of cracks at imprints (Fig. 8) in contrast to Cu/LiF CSs, which are ductile, without any destructions (Fig. 7).

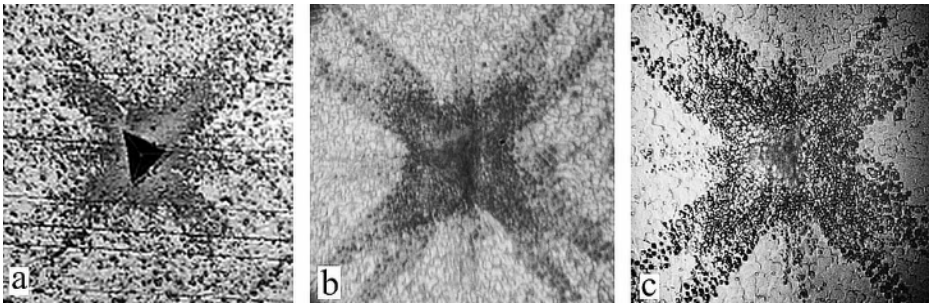

Fig. 7 – a) – The shape of dislocation rosettes appeared around the imprints on the LiF substrate after removing the copper film from the Cu/LiF structure; b, c) – type of dislocation rosettes after slight polishing of the surface of the LiF substrate; (a, b) – Cu/LiF, t = 85 nm; (c) – Cu/LiF, t = 470 nm; P [mN]: (a, c) – 500; (b) – 700. Zoom scale – the horizontal side of each image is 180 μm.

The contribution of the film thickness is manifested by the fact that the size of the dislocation rosettes, as well as the brittleness of the imprints, decrease with t increase (Fig. 8). The same effect was noted for Cu/Si CSs. In Figs. 9a, 9d, cracks and splits are visible, which have decreased in size in Figs. 9b, 9e and are absent in Figs. 9c, 9f, and a small pile-up formed near the imprint. As noted above, the dislocations on Si crystals are tightly pressed to the imprint due to a very low velocity and are detected only by TEM or by chemical etching after crystal annealing [25–27]. Since the dislocations are not able to transfer the material

inward and outward during the indenter introduction due to the low speed, the formation of imprints occurs mainly due to the phase transitions [25].

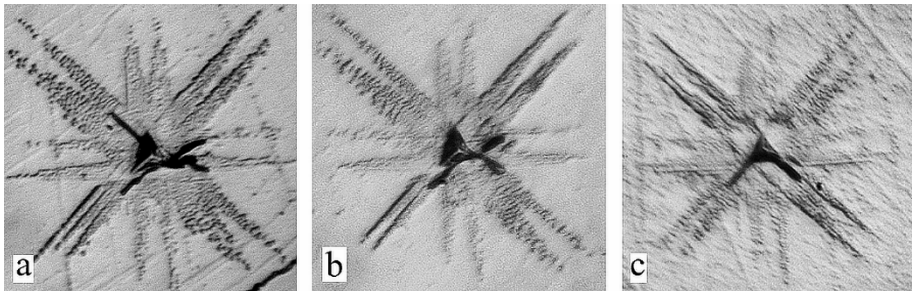

Fig. 8 – The shape of dislocation rosettes appeared around the imprints on the MgO substrate after removing the copper film from the Cu/MgO structures. a) – Cu/MgO, t = 85 nm; b) – Cu/MgO, t = 470 nm; c) – Cu/MgO, t = 1000 nm, P = 700 mN. Zoom scale – the horizontal side of each image is 150 μm.

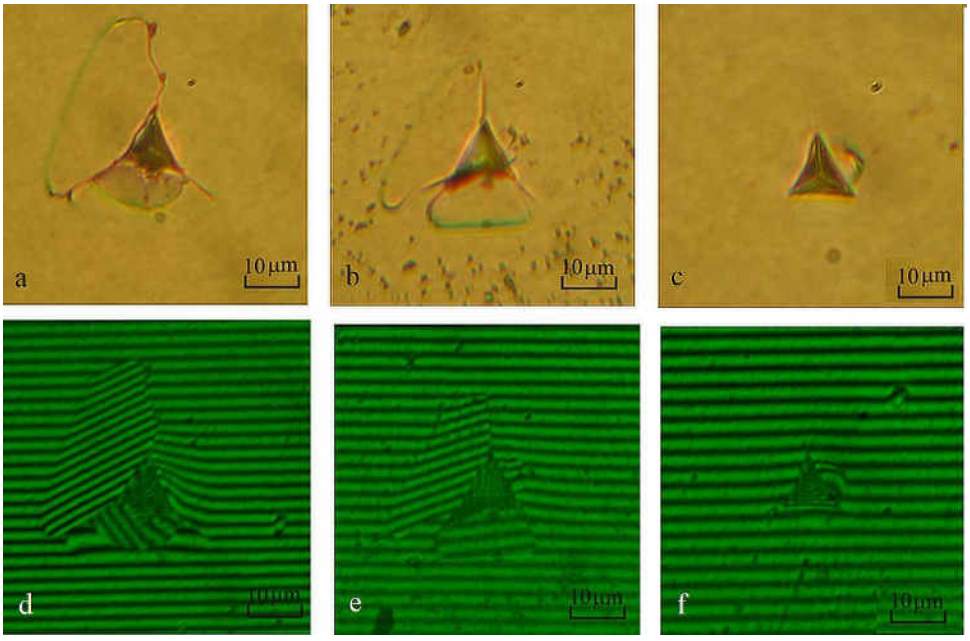

Fig. 9 – The shape of deformed zones appeared around the imprints on the Si substrate after removing the copper film from the Cu/Si structures: (a, d) – Cu/Si, t = 85 nm; (b, e) – Cu/Si, t = 470 nm; (c, f) – Cu/Si, t = 1000 nm. P = 900 mN; (a–c) – the images in the reflection mode; (d–f) – the images in the interference mode.

Thus, the studies performed have demonstrated that the mechanism of the imprint formation in LiF, MgO, and Si substrate crystals differs significantly, which leads to different mechanical responses of coated systems to an external load.

Different mechanical behavior of nanocomposite structures is a factor affecting parameters such as hardness, elasticity, plasticity index, resistance index, and tribological properties of the composite structure as a whole. The results obtained made it possible to explain the synchronous behavior of the H/E and H^3/E^2 curves. An increase in the plasticity index with the increase in film thickness and increase in load is quite natural, since at higher values of t, the contribution of the soft film to the deformation increases, and at higher values of P_{max}, the size of the deformed zone increases, increasing the plasticity of the CS. However, as it was mentioned above, the increase in the deformed zone is accompanied by its complication, the creation of a dislocation-disclination substructure, rotational transformations, and the emergence of new phase structures. These structures provide higher resistance to further deformation of the CS, which is manifested in an increase in the resistance index. Consequently, the analysis of the structure of the deformed zones in the CSs with different types of chemical bonding in the substrates reveals a new vision of the substrate response mechanism to the action of the external load.

5. CONCLUSION

This work studies the effect of various Cu/substrate systems (Cu/LiF, Cu/MgO, Cu/Si) on the change in the plasticity index H/E and the resistance index H^3/E^2 under indentation in a wide range of loads P_{max} = 5–900 mN. These structures have been formed based on the same soft material, a metal film (Cu, H = 0.6 GPa), but with different hardness and different types of chemical bonding in single crystal substrates: 1 – LiF, soft crystal, ionic bond type, SS_i; 2 – MgO, hard crystal, ionic-covalent bond type, SH_{ic}, and 3 – Si, hard crystal, covalent bond type, SH_c, the hardness of which is H = 1.2, 7.5, and 8.2 GPa, respectively. The plastic, strength, and wear-resistant properties of these CSs were compared. The main parameters of elasticity, plasticity and strength were determined, and the values of H/E and H^3/E^2 were also estimated. The microstructure and surface topography around indentations deposited on crystal substrates and on CSs were studied, strain curves $P(h)$ were analyzed, general and specific features of the nature of deformation and the response of coated systems to the action of a concentrated load were revealed.

It was shown that the difference in the behavior of the substrate crystals under the action of an external load is reflected in the values and behavior of the parameters of H/E and H^3/E^2. Thorough studies of the deformed structures of composite systems at the dislocation level made it possible to establish the mechanism of the CSs response to the action of an external load and to explain the specific feature of the plastic and strength properties of the coated systems such as “soft film/soft substrate” and “soft film/hard substrate”. By purposefully changing the CSs mechanical response, it is possible to obtain nanocomposite structures with required plastic and strength properties.

Acknowledgements. This work is supported financially by the National Agency for Research and Development of the Republic of Moldova under the grant no. 20.80009.5007.18.

REFERENCES

1. T.Y. Tsui, G.M. Pharr, W.C. Oliver, C.S. Bhatia, R.L. White, S. Anders, A. Anders, I. G. Brown, *Nanoindentation and nanoscratching of hard carbon coatings for magnetic disks*, Mat. Res. Soc. Symp. Proc. **383**, 447–452 (1995).
2. A. Leyland, A. Matthews, *On the significance of the H/E ratio in wear control: a nanocomposite*, Wear **246**, 1–11 (2000).
3. Z. Barbos, *Elastoplastic properties under nano-microindentation of phosphate glasses doped with rare-earth ions*, Mold. J. Phys. Sci. **18**(1–4), 53–58 (2019).
4. J. Musil, F. Kunc, H. Zeman, H. Polakova, *Relationships between hardness, Young's modulus and elastic recovery in hard nanocomposite coatings*, Surf. Coat. Tech. **125**, 322–330 (2000).
5. Y. Ren, L. Liang, Q. Shan, A. Cai, J. Du, Q. Huang, Sh. Liu, X. Yang, Y. Tian, H. Wu, *Effect of volumetric energy density on microstructure and tribological properties of FeCoNiCuAl high-entropy alloy produced by laser powder bed fusion*, Virtual and Physical Prototyping **15**(1), 543–554 (2020).
6. D. Tabor, *The Hardness of Metals*, Oxford University Press, London, UK, 1951.
7. D. Tabor, *The physical meaning of indentation and scratch hardness*, British J. Appl. Phys. **7**(5), 159–166 (1956).
8. K.L. Johnson, *Contact Mechanics*, 1st ed., Cambridge University Press, UK, 1985.
9. J.-H. Boo, M. J. Jung, H. K. Park, K. H. Nam, J. G. Han, *High-rate deposition of copper thin films using newly designed high-power magnetron sputtering source*, Surf. & Coat. Tech. **188–189**, 721–727 (2004).
10. D. Beegan, S. Chowdhury, M.T. Laugier, *The nanoindentation behavior of hard and soft films on silicon substrates*, Thin Solid Films. **466**, 167–174 (2004).
11. S. Suresh, T.-G. Nieh, B.W. Choi, *Nano-indentation of copper thin films on silicon substrates*, Scripta Mater. **41**(9), 951–957 (1999).
12. A. A. Volinsky, N. I. Tymiak, M. D. Kriese, W. W. Gerberich, J. W. Hutchinson, *Quantitative modeling and measurement of copper thin film adhesion*, Mat. Res. Soc. Symp. Proc. **539**, 277–290 (1999).
13. D. Grabco, C. Pyrtsac, O. Shikimaka, *Deformation under nano/microindentation of LiF, MgO, Si monocrystals stipulated as support materials for Cu/substrate structures*, Proceedings of ICNBME-2013, Chisinau, Moldova, 102–106 (2013).
14. D. Z. Grabco, C. M. Pyrtsac, O. A. Shikimaka, *Mechanical properties of polycrystalline copper and single-crystal LiF initial components for composite system Cu/LiF*, Surf. Eng. Appl. Electrochem. **52**(3), 233–241 (2016).
15. D. Z. Grabco, C. M. Pyrtsac, L. Z. Ghimpu, G.F. Volodina, *Mechanical properties of the coating/substrate composite system: Nanostructured copper films on a LiF substrate*, Surf. Eng. Appl. Electrochem. **52**(4), 319–333 (2016).
16. Daria Grabco, Constantin Pyrtsac, Olga Shikimaka, *Relaxation parameters of Cu/substrate type coated systems under nanoindentation*, IFMBE Proceedings. **5**, 55–61 (2022).
17. W.C. Oliver, G.M. Pharr, *An improved technique for determining hardness and elastic modulus using load and displacement sensing indentation experiments*, J. Mater. Res. **7**(6), 1564–1580 (1992).
18. J-il Jang, M. J. Lance, S. Wen, T. Y. Tsui, G. M. Pharr, *Indentation-induced phase transformations in silicon: influences of load, rate and indenter angle on the transformation behavior*, Acta Mater. **53**, 1759–1770 (2005).
19. R. Saha, W. D. Nix, *Effects of the substrate on the determination of thin films mechanical properties by nanoindentation*, Acta Mater. **50**, 23–28 (2002).
20. A. R. Shugurov, A. V. Panin, K. V. Oskomov, *Peculiarities of determination of mechanical characteristics of thin films by nanoindentation method*, PSS. **50**(6), 1007–1012 (2008).

21. A. M. Korsunsky, M. R. McGurk, S.J. Bull, T. F. Page, *On the Hardness of Coated Systems*, Surf. Coat. Techn. **99**, 171–183 (1998).
22. D. Grabco, B. Pushcash, M. Dyntu, O. Shikimaka, *Thermal evolution of deformation zones around microindentation in different types of crystal*, Phil. Mag. A **82**(10), 2207–2215 (2002).
23. D. Grabco, *Dislocation-disclination mechanism of deformation under microindentation*, Mold. J. Phys. Sci. **3**, 94–103 (2002).
24. D. Grabco, O. Shikimaka, E. Harea, *Translation–rotation plasticity as basic mechanism of plastic deformation in macro-, micro- and nanoindentation processes*, J. Phys. D: Appl. Phys. **41**, 074016 (9pp) (2008).
25. M. S. R. N. Kiran, T. T. Tran, L. A. Smillie, B. Haberl, D. Subianto, J. S. Williams, J. E. Bradby, *Temperature-dependent mechanical deformation of silicon at the nanoscale: Phase transformation versus defect propagation*, J. Appl. Phys. **117**, 205901 (2015).
26. E. Harea, *Deformation of TCO/Si planar structures under the action of concentrated load*, (in Romanian), PhD Thesis in Physics, Sciences, Chisinau, Moldova (2011).
27. D. Grabco, O. Shikimaka, E. Harea, C. Pyrtsac, *Visualization of undulatory mass transfer in near-surface vicinity of indentation contact zone*, 5th ICMSCMP, Chisinau, Moldova, 144 (2010).